Egypt. J. Phys. **Vol. 50,** pp. 25-45 (2022)

Egyptian Journal of Physics
http://ejfs.journals.ekb.eg/

Thermal Events and Microanalysis of New Complex Lithium-diphenyl Carbazide

F. El-Kabbany, M. Hafez* and N.R. Abdel Aziz
Physics Department, Faculty of Science, Cairo University, Cairo, Egypt

THERMAL properties and thermal events in lithium-diphenyl carbazide complex (LiDPC) are studied here by thermogravimetric analysis (TGA) and thermomechanical analysis (TMA). TGA showed a weight loss 4.1 % while TMA showed a slow shrinkage at 77 °C and then changes to a fast shrinkage above 80 °C with a shrinkage coefficient 47.3 μm/°C. The shrinkage phenomenon in LiDPC is found to be time dependent. The activation energy for the isothermal process is calculated and found to be 0.39 eV. A set of SEM photos of LiDPC complex are recorded and supported what is obtained by X-ray diffraction patterns. The I-V characteristics of lithium diphenyl carbazide (LiDPC) polycrystalline layers with thickness ranged from 150 to 1000 μm are studied and the critical voltage (V_C) and breakdown voltage (V_b) are evaluated. Heating effect of LiDPC samples shows a clear change in their electric current behavior near T_C = 60 °C.

Keywords: Joule heating, Lithium complex, Thermal events.

Introduction

Studying the features and structure of the thin layer metal-organic complexes gains a great interest [1-5], particularly in the field of microelectronics. Both scientific and technological points of view are of interest in such studies. The clarification of the physical characteristics of thin layers depends on complete knowledge of arrangement of atoms in the layers and information about the presence of the lattice defects which exist. As insulation for surface passivation between conductors and as dielectrics in condensers, thin insulating layers are sometimes used. The insulating layer must keep its dielectric properties with stress and time in most these applications. As a result, the electrical breakdown force was given much concern.

One of the important organic compounds in the field of analytical chemistry [6-8] is diphenyl carbazide (DPC). As shown by De Ranter [9], DPC ($C_{13}H_{14}N_4O$) has an orthorhombic crystal structure with the pbnm space group. On either side of a crystallographic symmetry plane, two phenyl hydrazide groups lie along the bond direction of the carbonyl group in this crystalline structure, Fig.1.

DPC inverts from orthorhombic crystal structure [9] to the amorphous structure at 162 °C (m.p). Previous work on DPC was describing the stability crystallography and thermodynamics of this organic compound [10-16]. The introduction of a metal ion, such as Li^+ ion into DPC lattice, a metal-organic complex is obtained with completely new features. LiDPC complex is prepared here under certain condition. The insertion of such electron rich metal element may give new structure and properties [17-19]. The structural properties of the DPC in relation to thermodynamic quantities have been reviewed and discussed [6].

A previous full IR survey and new results (at R.T and at 80 ºC) of crystalline, amorphous DPC and LiDPC was carried out and reported [20]. A completely new complex associated with new properties is created when the implementation of Li^+ ion into diphenyl carbazide $C_{13}H_{14}N_4O$. IR analysis included measurements and interpretation

*Corresponding author: marwa@sci.cu.edu.eg ; marwahafez111@yahoo.com
DOI :10.21608/ejphysics.2021.68549.1064
Received : 21/3/2021; accepted : 18/4/2021

of the IR spectral band shape, intensities and frequencies of the inner modes of vibrations. The crystal structure of LiDPC and its parameters were estimated using X-ray diffraction analysis. It is shown from X-ray analysis that LiDPC has a triclinic crystal structure with "a = 5.6929 Å, b = 7.6378 Å , c = 17.8739 Å, α = 119.176º, β = 63.322º, γ = 85.378º ". It is observed from the results the existence of an order–disorder phase transition in LiDPC complex at 60 ºC [20].

Our aim in this study is to exhibit the crystal structure of LiDPC. Is this a completely new organic complex with new properties or it is just a modification? It is of interest to try to give correct answers to these questions by achieving a set of analysis for LiDPC using thermal analysis (TGA and TMA), mass spectroscopy, NMR, and scanning electron microscopy (SEM).

I-V characteristics of LiDPC thin-layers are studied in this paper, taking account of the effect of heating and to show some forms of the breakdown properties in it. The scope of the work is further extended by studying insulating systems at high voltages, an approach that has been very rewarding. It is hoped that this approach is equitably appropriate for the manufacture of electronic components and microelectronic devices.

Experimental details

"From the British Drug House (BDH), Laboratory Chemical Division", England, ultra pure diphenyl carbazide (DPC) powder was used. LiDPC compound sample is prepared by a chemical reaction between amorphous DPC and lithium nitrate (dissolved in acetone)

$$C_{13}H_{14}N_4O + LiNO_3 \rightarrow C_{13}H_{13}N_4OLi + HNO_3$$

After few days, a brown precipitated crystallites is obtained. The physical properties of this new organic compound can be studied after precipitation and drying.

Thermal analysis (TGA and TMA), the Shimadzu system type 60 made in Japan, was carried out in this study. A quaderpole mass spectrometer was used to study the mass spectrum of the LiDPC (type Shimadzu Qp-2010 plus, Japan). The ions are generated at 70 eV by electron impact at the source of the ion. The vaccine operation, which relies on the vapor pressure of the sample, was 10^{-4} Torr. About 250 ^{o}C was the temperature of the ion source. NMR analysis using DMSO solvent was obtained using a Bruker instrument (500 MHz ultra shield).

The scanning electron microscopy (SEM) study is carried out using Joel scanning electron microscope made in Japan. The low electric current measurements are performed here by an auto ranging picometer (Type KEITHLEY 485 capable of measuring range from 2 nA to 2 mA with resolution from 0.1 PA to 100 nA respectively) and good insulation precautions are taken into account so as to preserve this capability.

Results and Discussion

Thermal stability of LiDPC

Figure 2 shows TGA for LiDPC sample. TGA is often used to detect the thermal stability of samples and to reveal decomposition profiles for weight loss. Moreover, Fig. 2 shows typical thermal profile for LiDPC. One can see that there is a weight loss 4.1%. TGA analysis demonstrates considerable weight loss over a wide range of temperature. This loss is likely to be due adsorbed moisture at material surface or held to it by weak attractive forces.

Figure 3 shows the thermodilatometric or thermomechanical analysis (TMA) of LiDPC sample. No dilatation change could be detected during heat increase up to ≈ 77 ^{o}C. As the temperature exceeds this value, slow shrinkage takes place followed by sudden fast shrinkage above 80 ^{o}C. The shrinkage coefficient is 47.3 µm/ ^{o}C. Also Fig. 3, shows a highly accurate dilatometric measurements for LiDPC sample. The observed sudden change in sample length ΔL (shrinkage state) was retained with further heating. This figure shows an obvious contraction behavior during increasing of the temperature 5 ^{o}C/ min in the temperature range (40-120 ^{o}C). The contraction begins sharply at ≈ 77 ^{o}C and reveals a sudden variation as the temperature increases up to 120 ^{o}C. The relation between ΔL against T is a non-linear. It is reported that the semielastic behavior depends on the time lag before the reheating measurements [21]. Such behavior shows the necessity to study the dependence of contraction on time as shown in Fig. 4. It is noticed that the shrinkage is time dependence at low temperature and is reduced as the temperature increased.

LiDPC studies have been conducted to obtain the activation energy of the isothermal process. For the calculations used, a set of results is provided below. Figure 4 shows time dependence at

different temperatures for the dilatometric change. It is clear that ΔL continually decreases before a certain time interval reaches an almost constant value. In order to achieve its constant value, the ΔL was found to require fewer rinsing periods at high temperatures. This behavior suggests that the observed change in ΔL term might be attributed to some thermally activated process. The process may be controlled by a rate equation which can control the process in the form [22].

$$t \exp(-\Delta E/kT) = \text{constant},$$

where ΔE is the activation energy, T is the temperature, t is the time and k is Boltzmann's constant.

Figure 5 exhibits the variation of lnt with the reciprocal of the temperature. The average value for the activation energy of the isothermal process is calculated and is found to be 0.39 eV.

I-V characteristic graph of the LiDPC sample is shown in Fig. 6 in the form of a thin layer of thickness 150 μm. It is noticed from the figure that there are two straight lines of different slopes. The slope kink begins at a critical voltage (V_C) (about 30 V). When the applied voltage increases, a breakdown voltage (V_b) is obtained where there is abrupt increase in electrical current. When the applied voltage across the sample is increased above a certain level, the insulating layer is locally destroyed and the capacitor is, at least temporarily, short-circuited. This is a well-known phenomenon in general dielectrics [23]. There are different models have been provided for such phenomena [24-26]. Two different mechanisms control the current at the V_C and the V_b. This will later be clarified and discussed. Figure 7 shows I-V characteristics of LiDPC thin layers at various thicknesses (200 - 1000 μm). It is obvious that there is a specific V_C and V_b for each studied thickness. Figure 8 shows the variation of V_C with the sample thickness.

The dependence of d.c. current on Joule heating

The relationship between the current and the voltage is straight lines up to a certain voltage after the common ohmic range, according to Fig. 9. Above the critical voltage V_C, the behavior is straight line with increasing in slope. This behavior proposed increase in current as applied voltage exceeded a critical value V_C may be due to the possibility of Joule heating. In order to interpret the results it was necessary to make some assumptions.

As shown in Fig. 9, the results fit into a square law at voltages less than V_C. At a voltage greater than V_C, the electrical current is assumed to increase from I_1 to I_2 corresponding to an increase in the sample temperature from T_1 to T_2, whereas under $V < V_C$, the steady current is assumed to have a value of I_1 at the temperature of layer T_1. $T_1 \neq T_o$, where T_o is the temperature of the room, must be noticed. Hence;

$$I_2 = a\, V^2 \exp\left(\frac{-\phi}{2kT_2}\right) \quad (1)$$

$$I_1 = aV^2 \exp\left(\frac{-\phi}{2kT_1}\right) \quad (2)$$

where "a" is a constant.

Here, an exponential temperature dependence with activation energy φ is assumed, then;

$$\ln\left(\frac{I_2}{I_1}\right) = \frac{-\phi}{2k}\left(\frac{1}{T_1} - \frac{1}{T_2}\right) \quad (3)$$

Suppose a simple form cooling law

$$I_2 V_2 = M (T_2 - T_o) \quad (4)$$

where I_2V_2 is the energy per second and M is a constant.

The thermal breakdown of insulators has been discussed with similar approach [27].

We have replaced T_2 from equation (4) to equation (3)

$$\frac{1}{\ln(I_2/I_1)} = \frac{2kT_1}{\phi}\frac{(I_2V + MT_o)}{(I_2V + M(T_o - T_1)} \quad (5)$$

When $T_1 = T_o$, then equation (5) becomes

$$\frac{1}{\ln(I_2/I_1)} = \frac{2kT_o}{\phi} + \frac{2kT_o^2M}{\phi}\left(\frac{1}{I_2V}\right) \quad (6)$$

A straight line is represented by the above equation (6). The new equation is obtained by multiplying both sides of the equation (6) with (I_2V),

$$\frac{I_2V}{\ln(I_2/I_1)} = \frac{2kT_o}{\phi} I_2V + \frac{2kT_o^2M}{\phi} \quad (7)$$

When data are entered in equation (7), the results are satisfactory in line (Fig.10). The pitch allows for a calculation of activation energy by φ = 0.17eV. Hence the deduction of M is possible.

Consider (I_2V) as the corresponding critical power in the assessment of T_C temperature at critical voltage of the V_C. Then from Eq. (4)

$$(I_2V)_c = M\,(T_C - T_o)$$

where the critical temperature equals to ≈ 60 °C.

The current at a constant voltage was measured according to the temperature, in order to gain an understanding of the importance of T_C.

Figure 11 shows the variation of the current of the layer with the change of the temperature where T_C is known as a temperature of phase transition which equals to 60 °C. The differential scanning calorimetry (DSC) curve carried out for LiDPC [20], in which obvious phase transition is detected at 62 °C, provides excellent confirmation of this assumption. Initiative examination of the I-V data which are reported indicates that Joule heating is a common property of I-V characteristic on electroluminescence [28, 29].

The value of critical power $(I_2V)_c$ varies significantly depends on the property of sample. It is associated with the change in M. Due to the existence of Joule heating effect that changes in the LiDPC complex compound's electrical properties are due to phase change as the applied voltage is increased. It is obvious that from studying I-V characteristics of the LiDPC complex that it is affected by Joule heating, which causes sample phase transition.

Breakdown characteristics

The detailed steps in LiDPC samples for breakdown phenomena are illustrated in Fig.12. It is evident that when the voltage is increased above V_C, the change of current up to the knee of the curve remains extremely small. The breakdown effect begins at this point. When the current increases sharply, the resistance of sample begins to decrease. The breakdown voltage V_b from the bottom of the knee remains essentially a constant voltage across its terminals over a specified range of the voltage used. I_a is maximum value of the current of the sample and I_b is the minimum

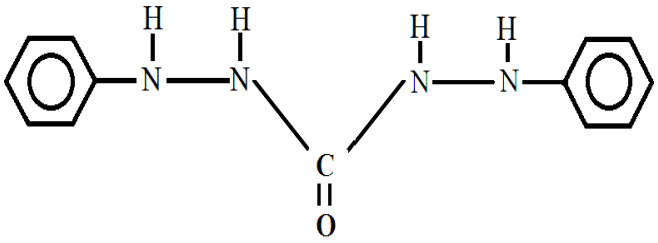

Diphenyle carbazide $C_{13}H_{14}N_4O$

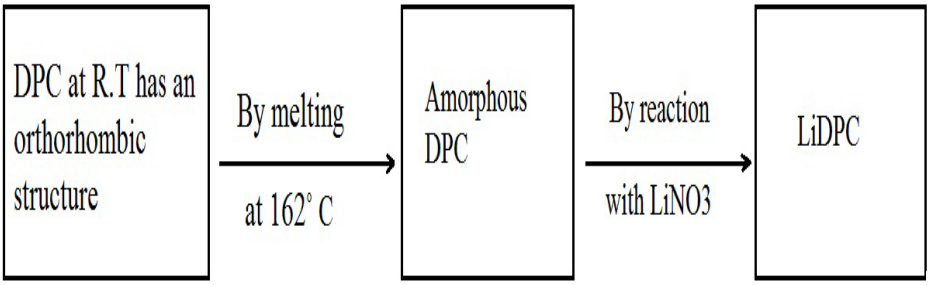

Fig. 1. DPC and LiDPC formation.

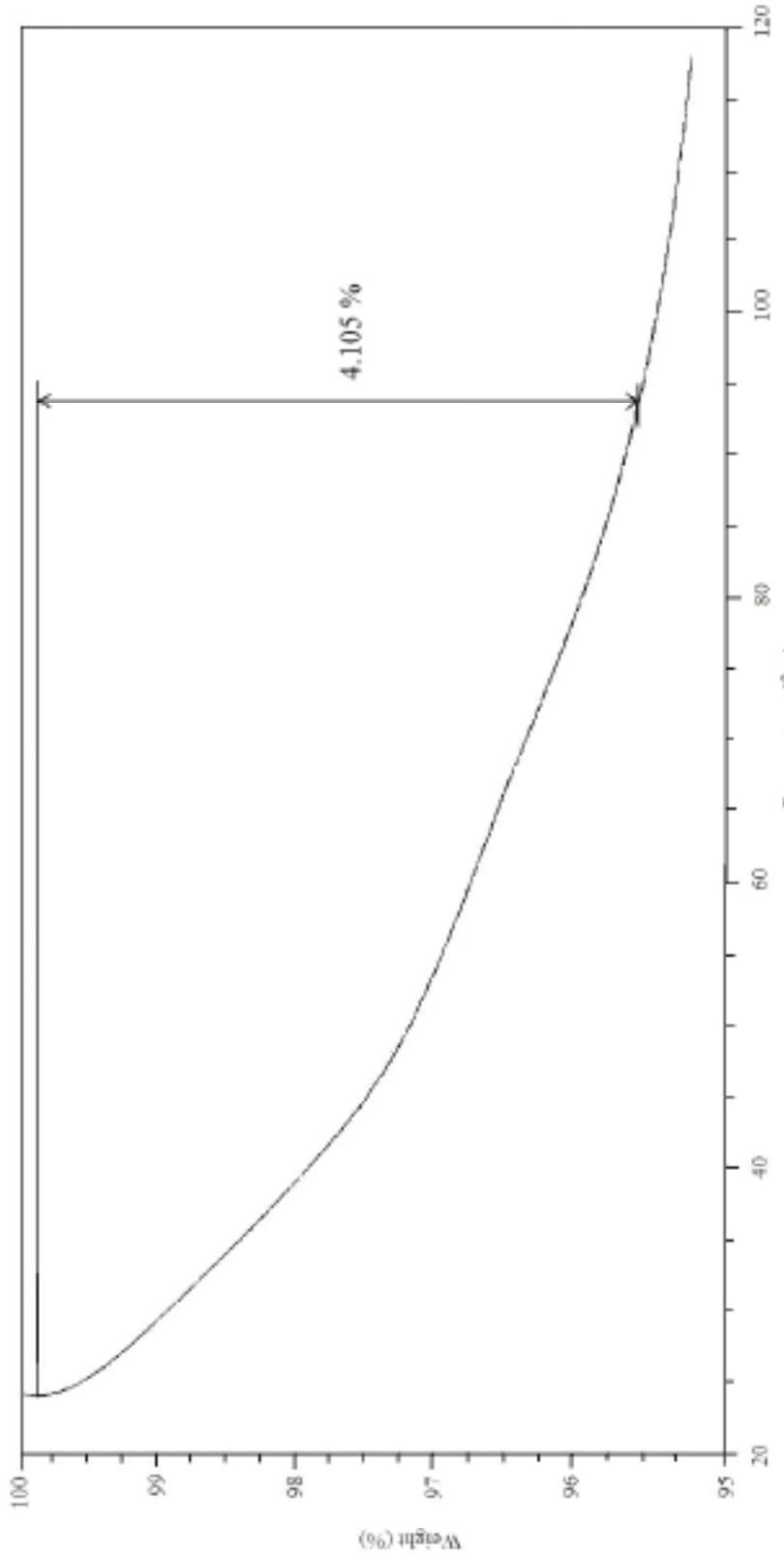

Fig.2 Thermogravimetric analysis of LiDPC sample.

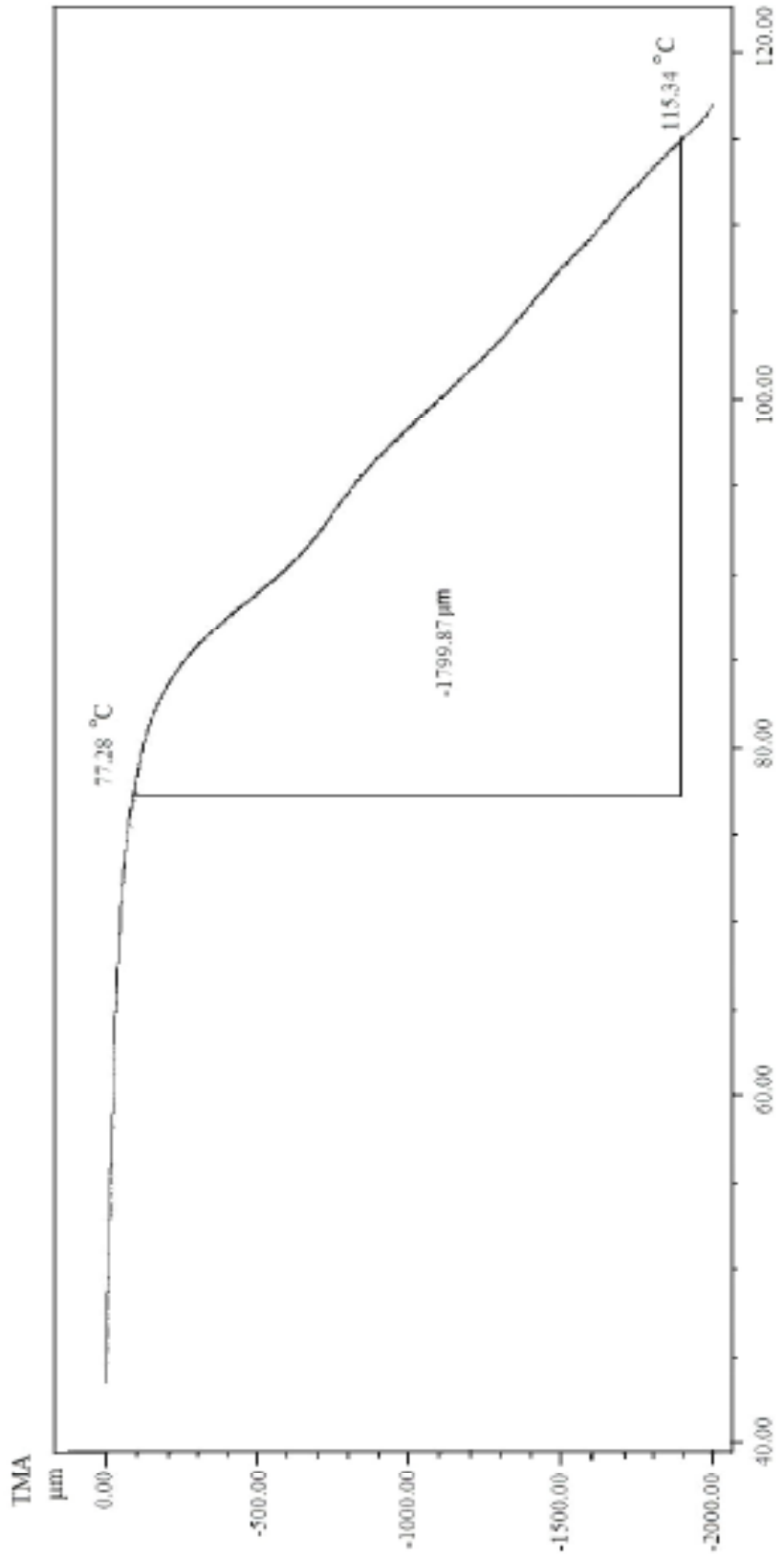

Fig.3 Thermodilatometric analysis of LiDPC sample.

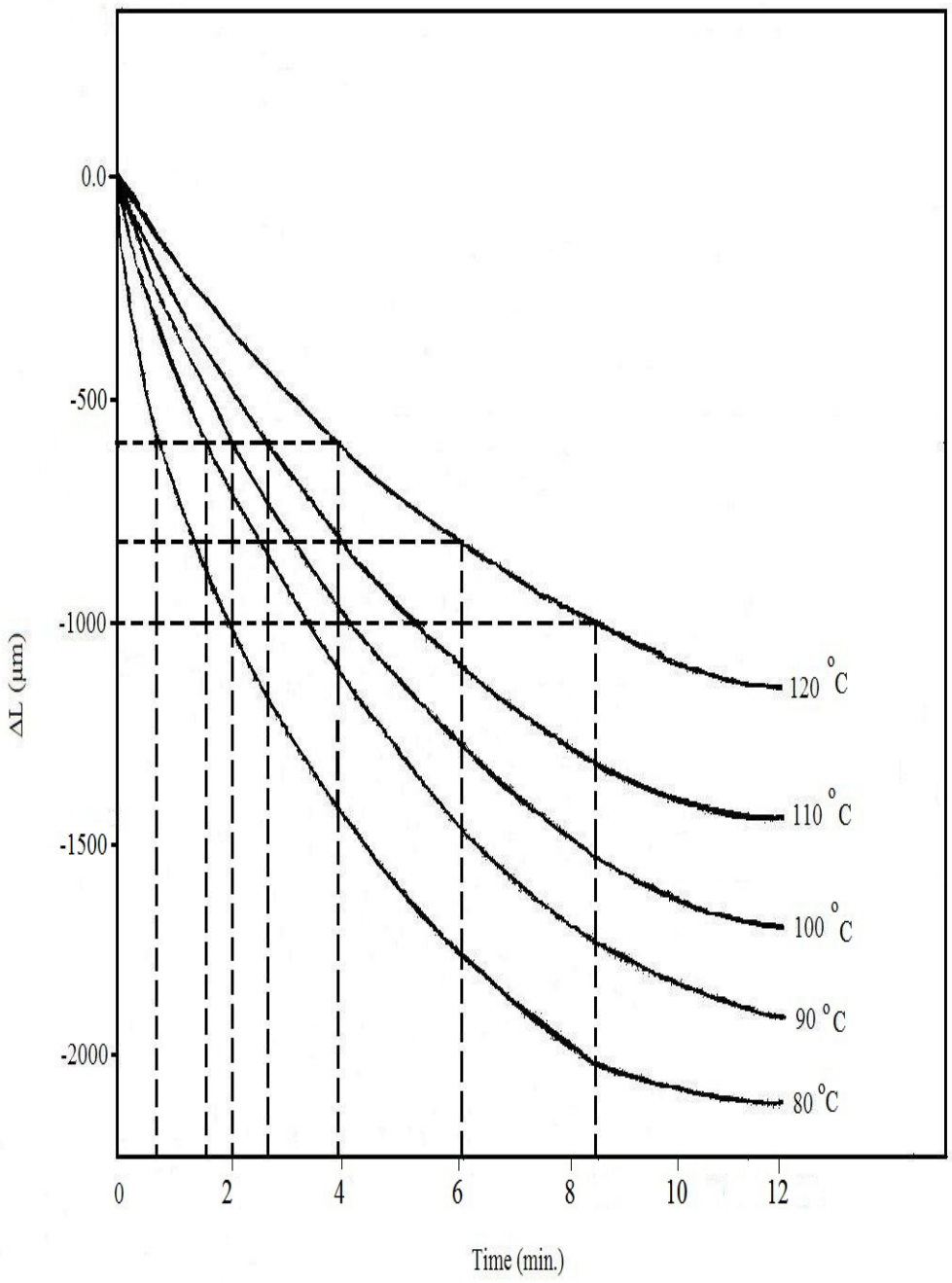

Fig.4 Variation of shrinkage of LiDPC samples with time.

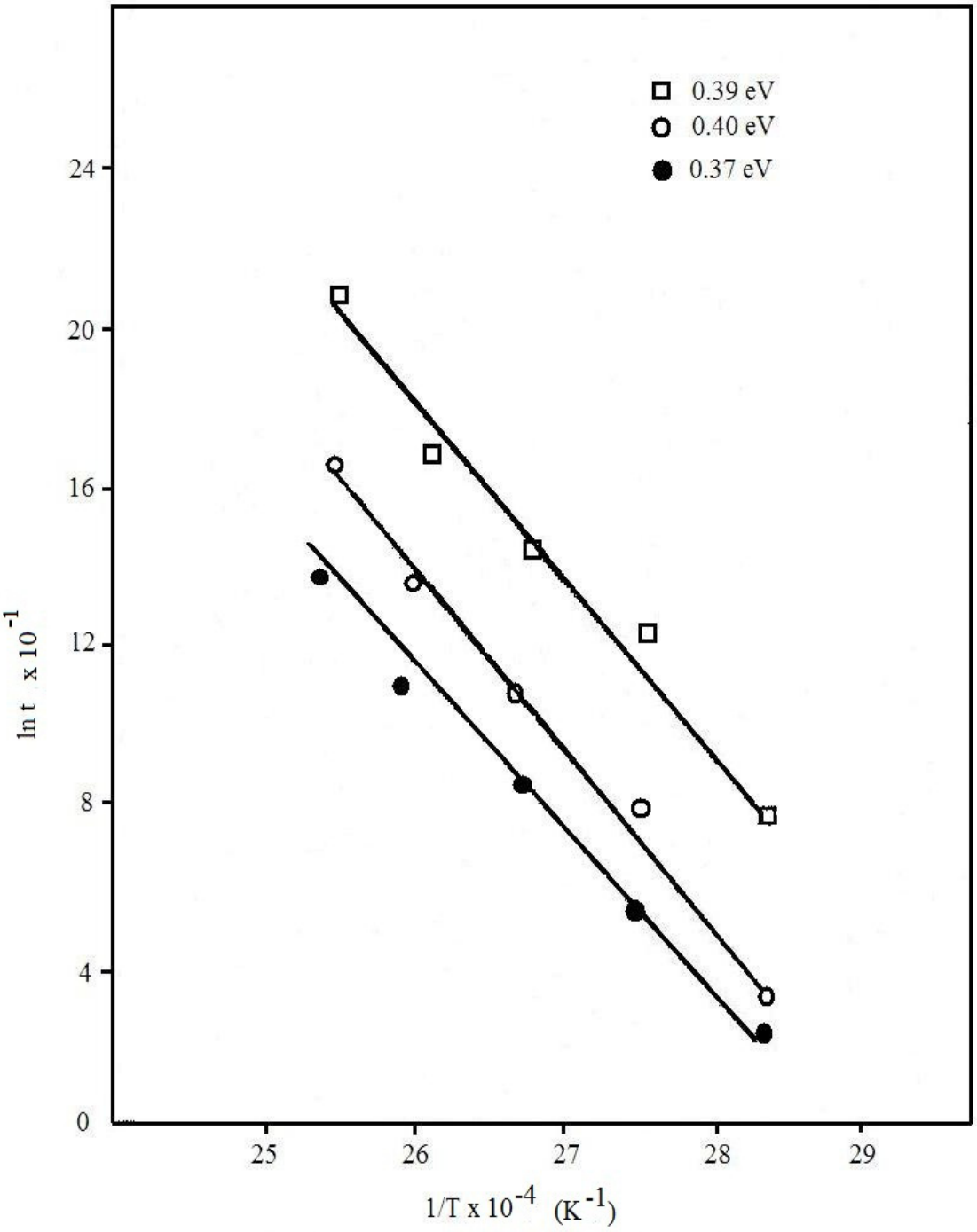

Fig.5 Variation of ln of annealing time versus the reciprocal of the absolute temperature.

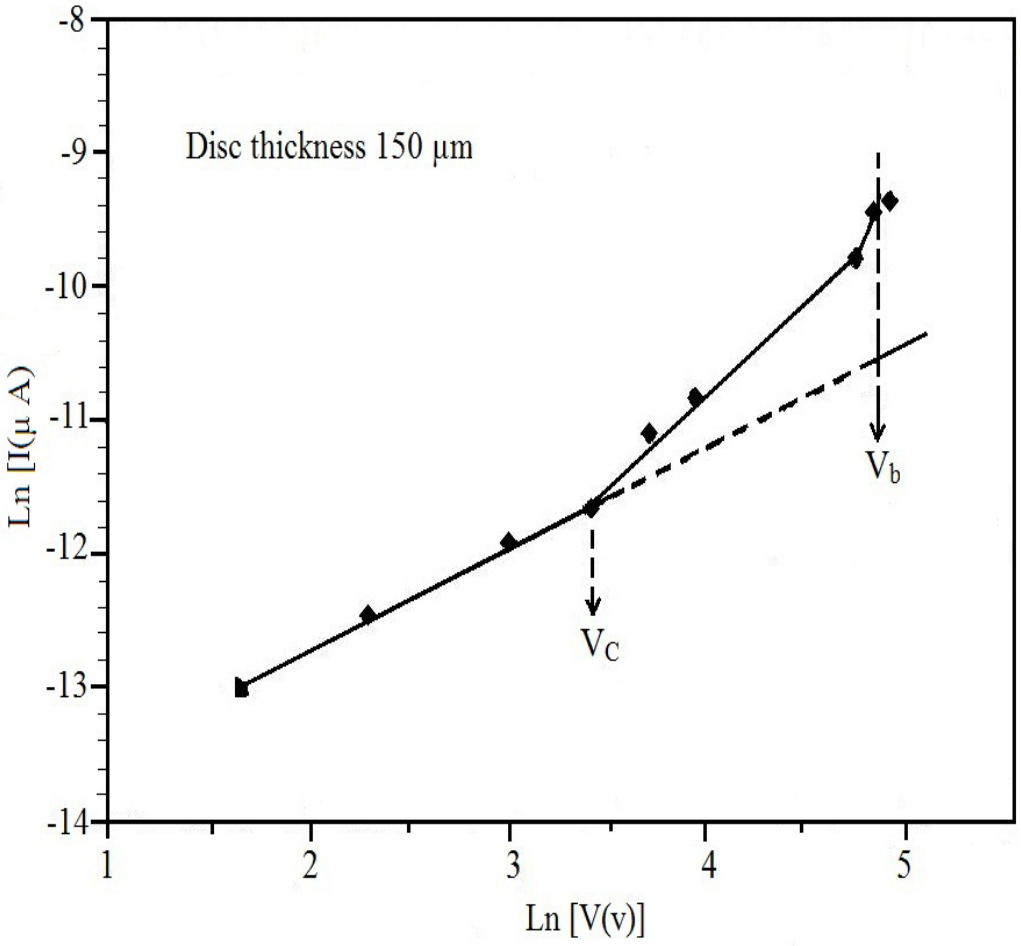

Fig.6. Graph of ln (I)-ln (V) characteristic of LiDPC sample.

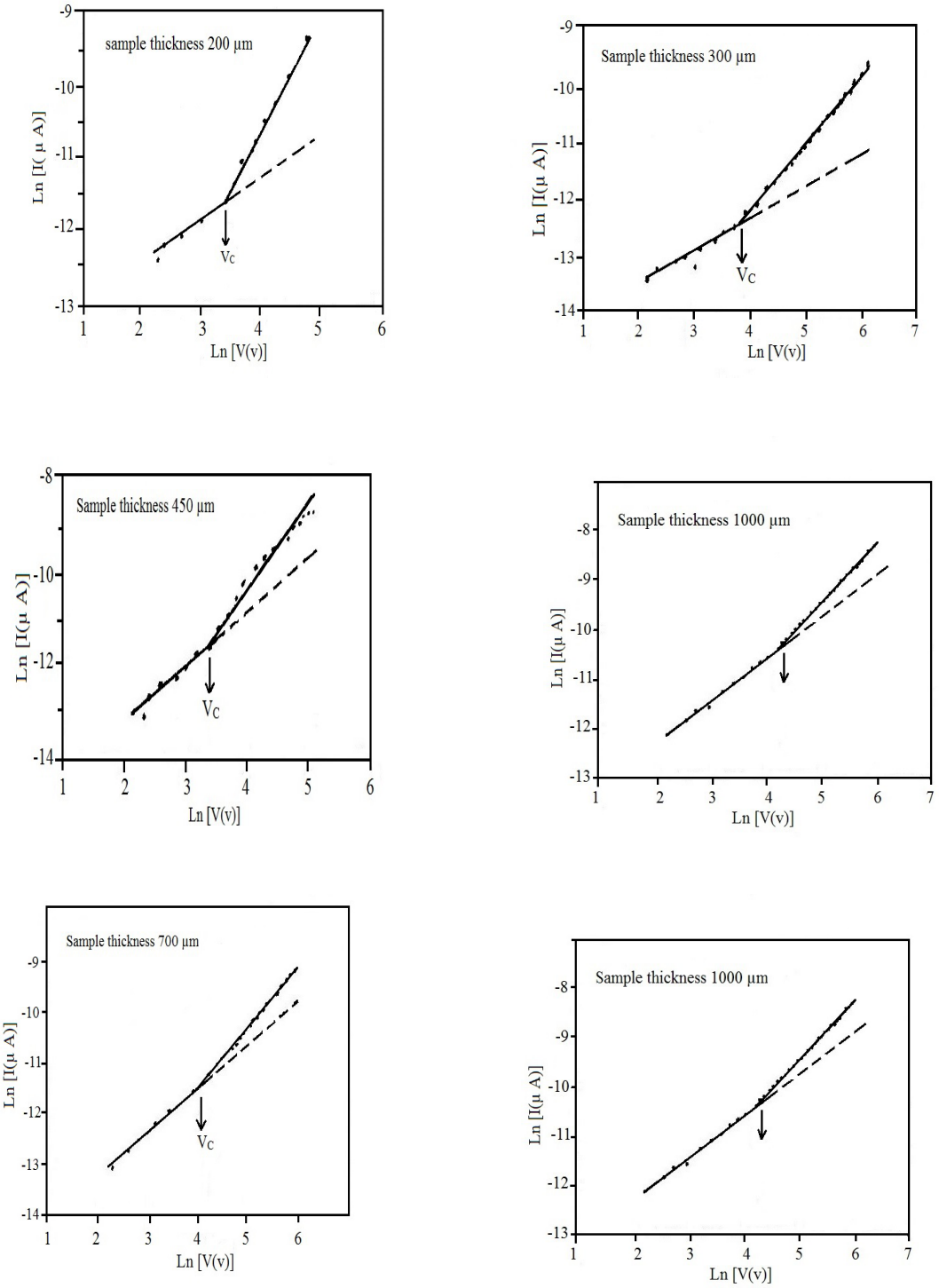

Fig.7. Graph of ln (I) - ln (V) for LiDPC thin discs of various thicknesses.

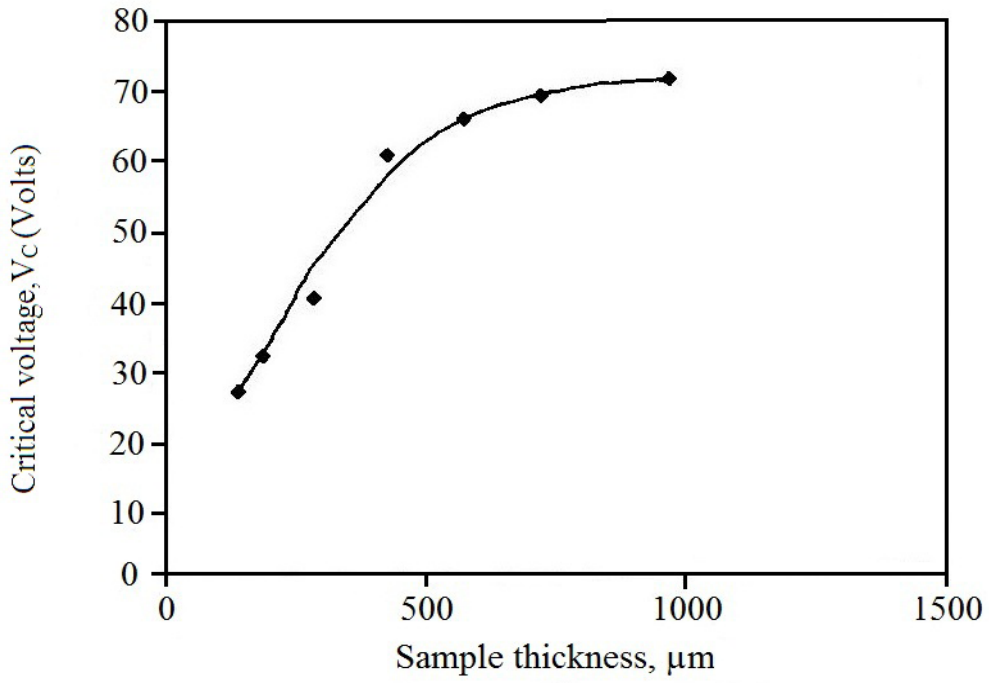

Fig.8. Variation of critical voltage V_C with sample thickness.

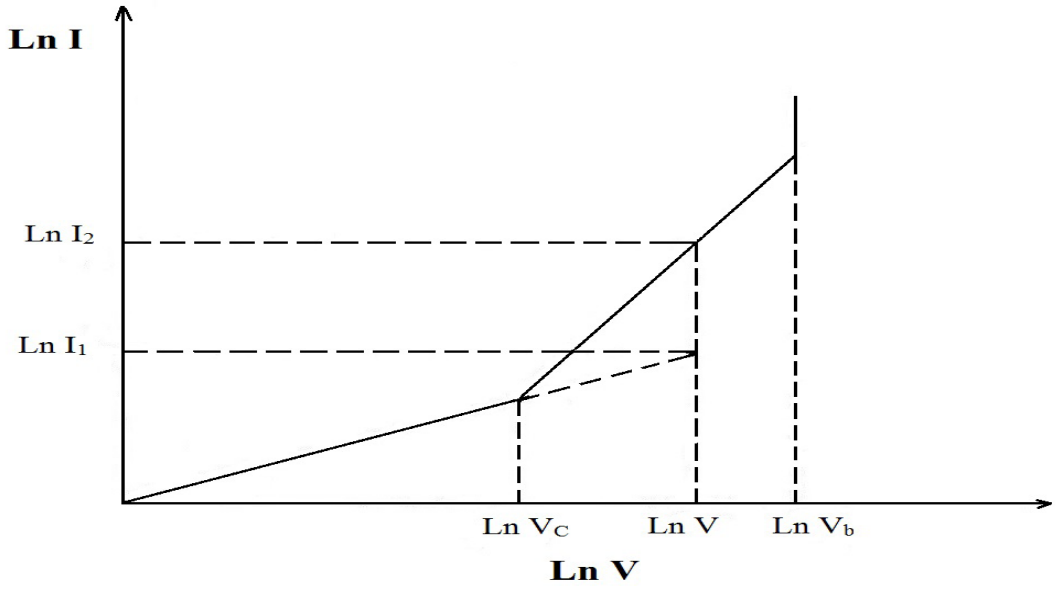

Fig. 9. Schematic form of ln I-ln V characteristic.

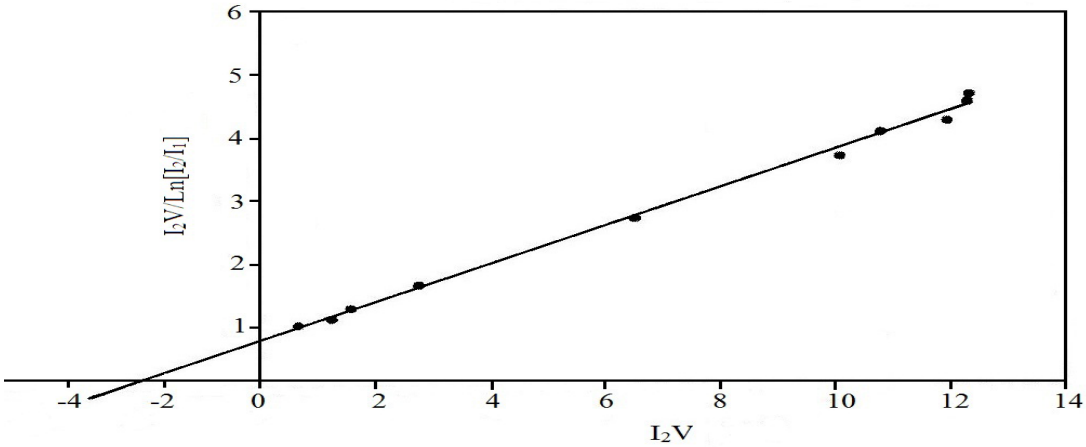

Fig. 10. Graph to test Joule heating assumptions, using Newton›s law of cooling.

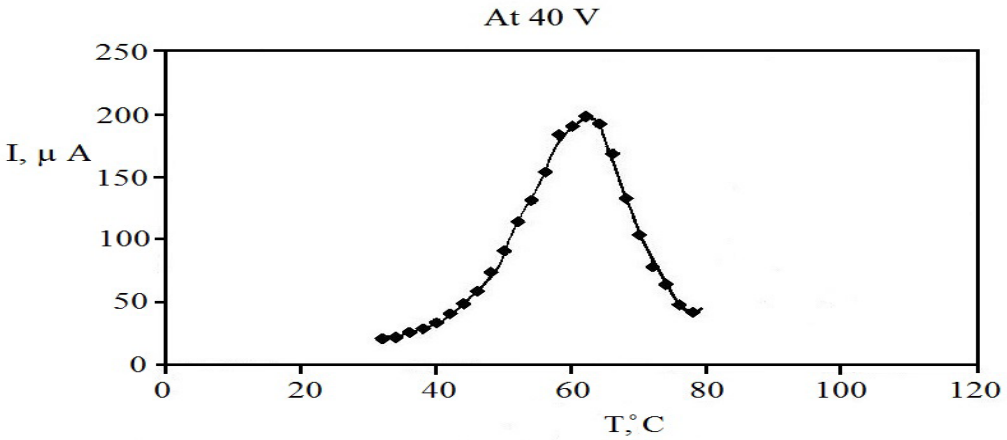

Fig. 11. Variation of the electric current with temperature for LiDPC sample.

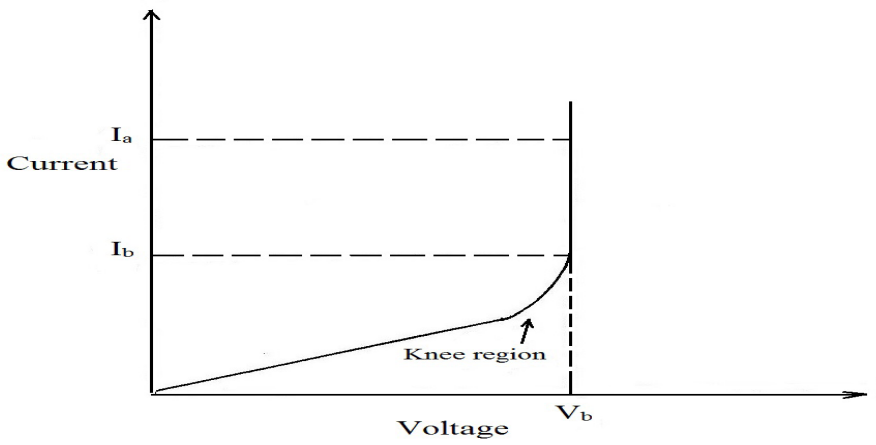

Fig. 12. Breakdown characteristics of LiDPC.

value of the breakdown current. When the sample current exceeds I_a, the sample may be damaged.

It is possible to explain the breakdown process through this dielectric material (LiDPC) as follows. A surface discharge over the insulator occurred at a lower voltage than across a straight-forward gap when electrodes are separated by a insulating material [30]. Free electrons are emitted at the cathode-insulator junction and these electrons strike the anode or insulator near the anode, thus releasing secondary electrons. A positively charged area near the anode moves towards the cathode on the surface of the insulator so that the stress increases to cause breakdown at the cathode.

Microanalysis of LiDPC complex

In the present study, the nature of the new complex LiDPC crystalline structure is also shown. Is the organic compound completely new or is it a phase of DPC?. A number of highly accurate analyzes of LiDPC samples using mass spectroscopy and NMR attempt to obtain a report and answers to these questions.

It is well known that molecular ions are commonly created in various electronically excited states when polyatomic molecules are ionized in gas phase by electron impact. When the number of atoms increases, by a series of radiationless transitions, the number of states can convert to highly vibrationally excite low-lying electronic state states, including the ground state. Thus, along numerous competitive reaction pathways, fragmentation can occur. The relative abundance of fragment spectra (Fig. 13) reflects the change over a large energy interval in the internal energy distribution. The comparative intensity of the fragments and the deterioration of the molecular ions in the ion source are shown in Table (1). The most intense peak is that fragment m/z = 93 ($C_6H_5NH_2$) which is noticed in mass spectrum of LiDPC which is found as a base peak. This ion is formed to produce two ions of the type $C_6H_5NH_2$ due to the bond dissociation of CN_2O_2 from the molecular ions on both its sides. On the other hand, with a relative intensity of 8.16 percent, the molecular M^+ has low absorbance. The spectrum also shows the existence of $(M+4)^+$ with a relative intensity of 10.1% .

According to the present mass spectra analysis for LiDPC, molecular weight is found to be 246. The calculated molecular weight is 248. This difference between the calculated value and that of mass spectra may be due two hydrogen atoms will be lost. This view point has been checked and confirmed by NMR (Fig.14).

According to the microchemical analysis (Table 1, Fig.13&14), the general molecular formula of the LiDPC compound under investigation can be given as $C_{13}H_{13}N_4Li$. The conclusive result of this mass analysis and NMR donates a molecular weight of LiDPC (246) that is completely different of the parent molecules (242 for DPC). This means that introducing Li^+ into DPC molecule leads to a new organic metal complex compound.

Figure 15 shows X-ray diffraction pattern of DPC sample at room temperature. Photo 1 shows an example of this orthorhombic crystal structure with magnification X = 1500 at 10 KV.

X-ray diffraction of DPC in its amorphous state as shown in Fig. 16. This diffraction pattern clearly indicates the non-crystalline structure (amorphous state) of this sample under test [20]. Photo 2 shows an SEM micrograph of some grains of DPC in its amorphous state at magnification X = 11000. Both of the X-ray diffraction and this SEM micrograph supports each other and indicates the presence of amorphous state of the parent or starting material (amorphous DPC). When lithium nitrate reacts with amorphous DPC, the new product obtained is LiDPC organic complex. Fig. 17 shows an X-ray diffraction of LiDPC complex sample [20]. This diffraction pattern indicates the presence of new crystal structure. Powerful crysfire program is used here to detect the crystal structure of a new complex. The results obtained by the computer analysis showed a triclinic structure with a = 5.6929 Å, b =7.6378 Å and c = 17.8739 Å, $\alpha = 119.176^o$, $\beta = 63.322^o$ and $\gamma = 85.378^o$ [20]. Photo 3 shows SEM micrograph of this triclinic crystal structure of LiDPC sample at magnification X = 2700.

The present measurements in this work are clearly evidence that insertion of Li ions into DPC molecules is accompanied by considerable changes in thermal properties and crystal structure. According to the present results, it is

TABLE 1. Mass table for the mass spectra of LiDPC by electron impact at 70 eV.

Peak no.	z/m	Abs. In	Rel.Int.	Peak no.	z/m	Abs.In.	Rel.Int.
1	50.00	132	17.10	35	122.00	58	7.51
2	51.00	255	33.03	36	123.00	57	7.38
3	52.00	119	15.41	37	128.00	55	7.12
4	53.00	76	9.84	38	133.00	95	12.31
5	54.00	57	7.38	39	134.00	105	13.60
6	58.00	71	9.20	40	136.00	73	9.46
7	60.00	60	7.77	41	139.00	63	8.16
8	61.00	81	10.49	42	148.00	66	8.55
9	62.00	60	7.77	43	149.00	62	8.03
10	63.00	92	11.92	44	151.00	119	15.41
11	64.00	127	16.45	45	154.00	60	7.77
12	65.00	345	44.69	46	162.00	89	11.53
13	66.00	74	9.59	47	171.00	65	8.42
14	69.00	76	9.84	48	173.00	52	6.74
15	75.00	58	7.51	49	183.00	74	9.59
16	76.00	110	14.25	50	184.00	58	7.51
17	77.05	644	83.42	51	185.00	70	9.07
18	78.00	175	22.67	52	191.00	60	7.77
19	79.00	94	12.18	53	197.00	52	6.74
20	80.00	103	13.34	54	200.00	63	8.16
21	81.00	66	8.55	55	206.00	60	7.77
22	90.00	55	7.12	56	210.00	63	8.16
23	91.00	94	12.18	57	213.00	66	8.55
24	92.00	310	40.16	58	215.00	70	9.07
25	93.05	772	100.00	59	217.00	52	6.74
26	94.00	124	16.06	60	220.00	55	7.12
27	96.00	52	6.74	61	227.00	70	9.07
28	99.00	58	7.51	62	234.00	54	6.99
29	102.00	74	9.59	63	236.00	52	6.74
30	104.00	89	11.53	64	240.00	54	6.99
31	105.00	94	12.18	65	242.00	63	8.16
32	107.00	334	43.26	66	245.00	103	13.34
33	108.00	338	43.78	67	246.00	78	10.10
34	121.00	54	6.99				

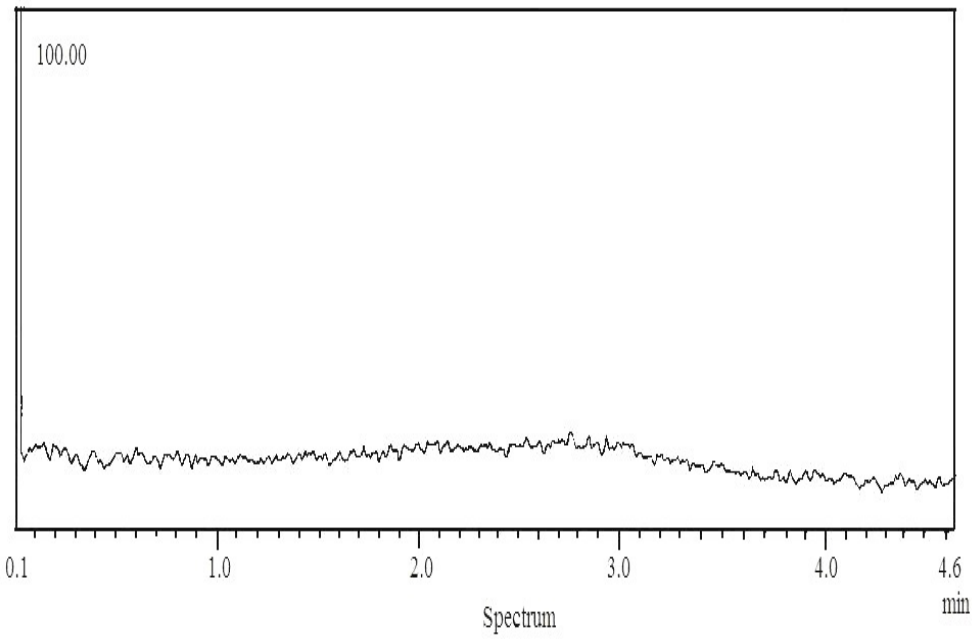

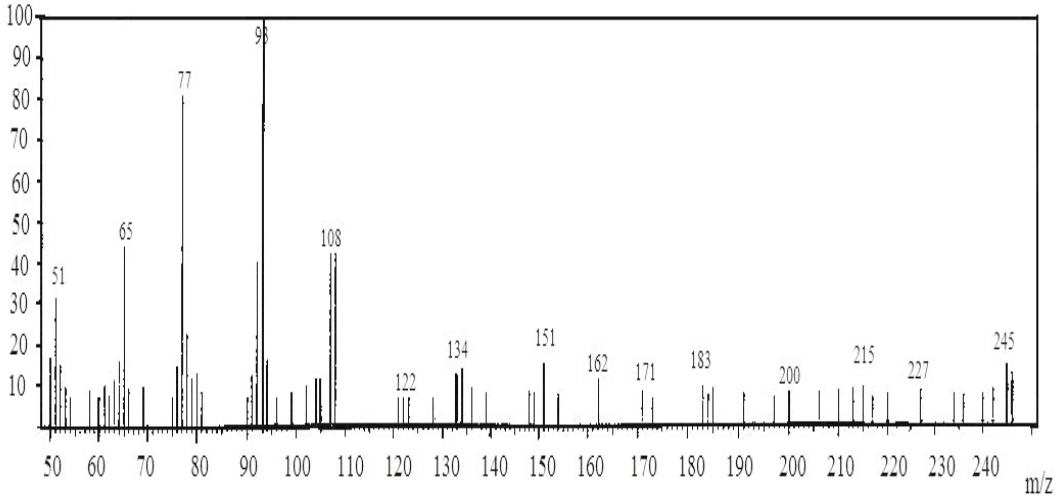

Fig. 13 Mass spectra of LiDPC at 70 eV.

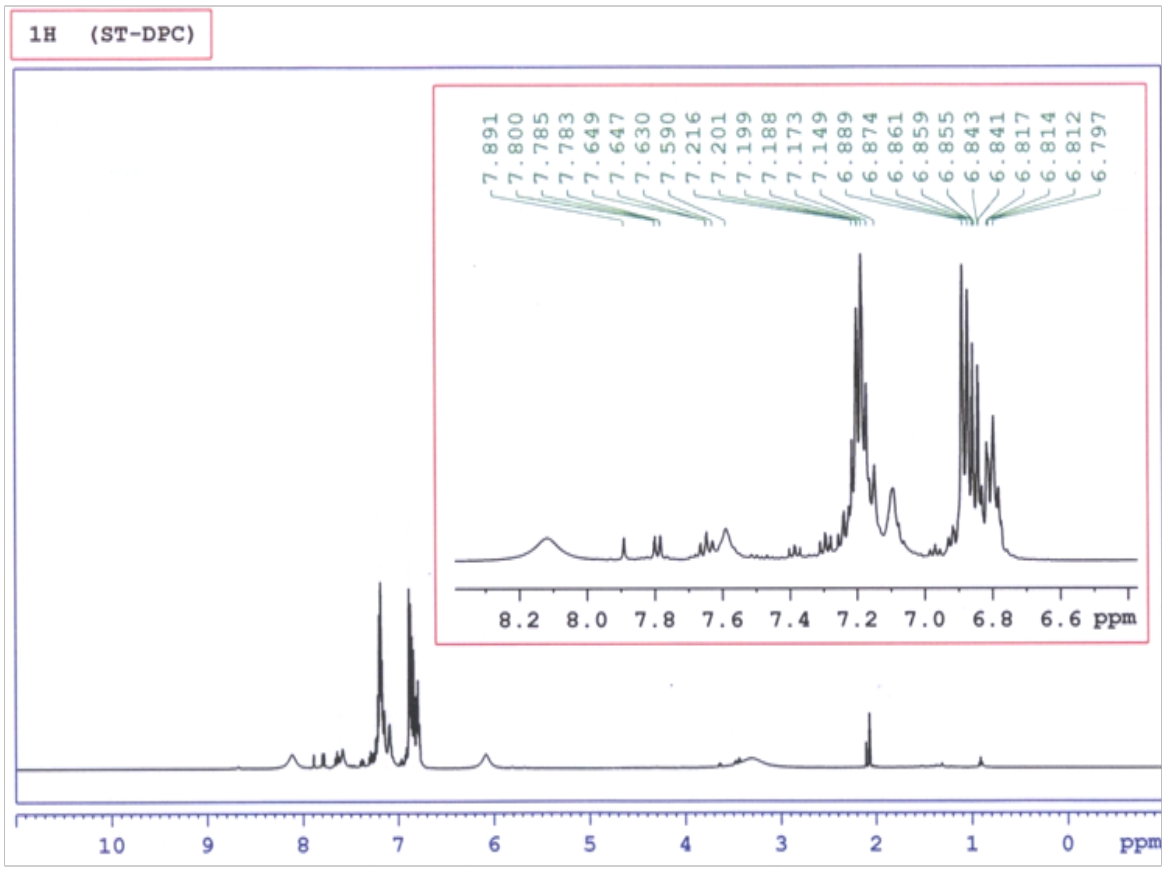

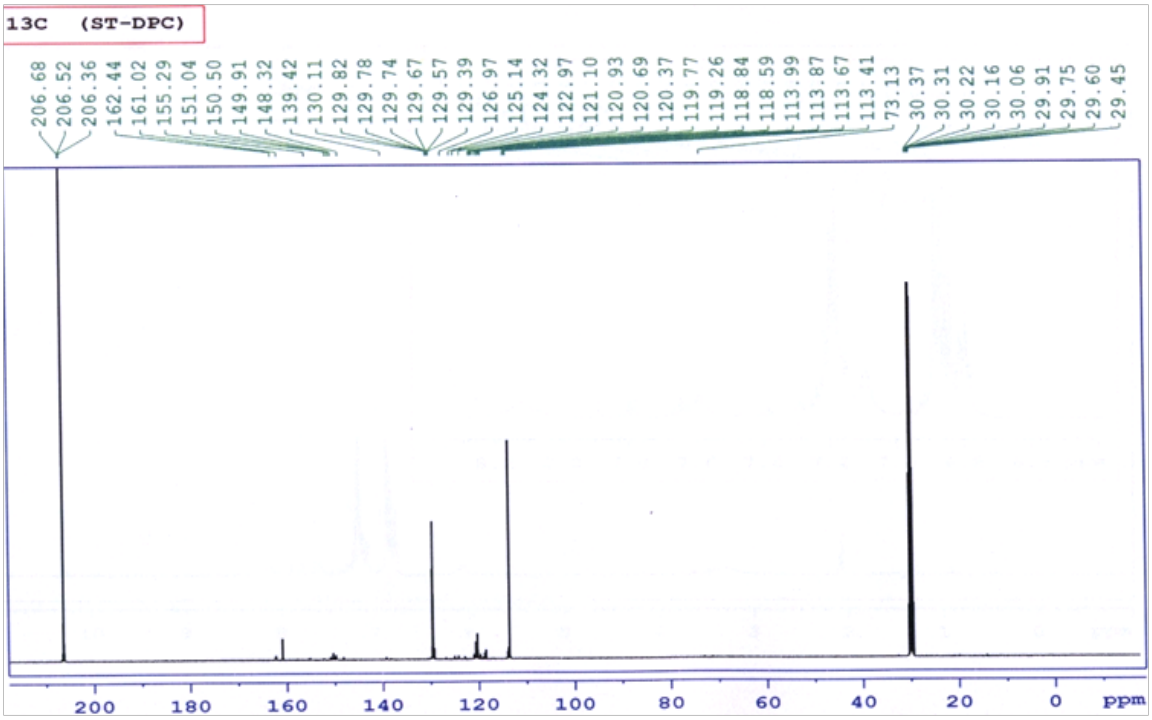

Fig. 14 NMR spectra of LiDPC.

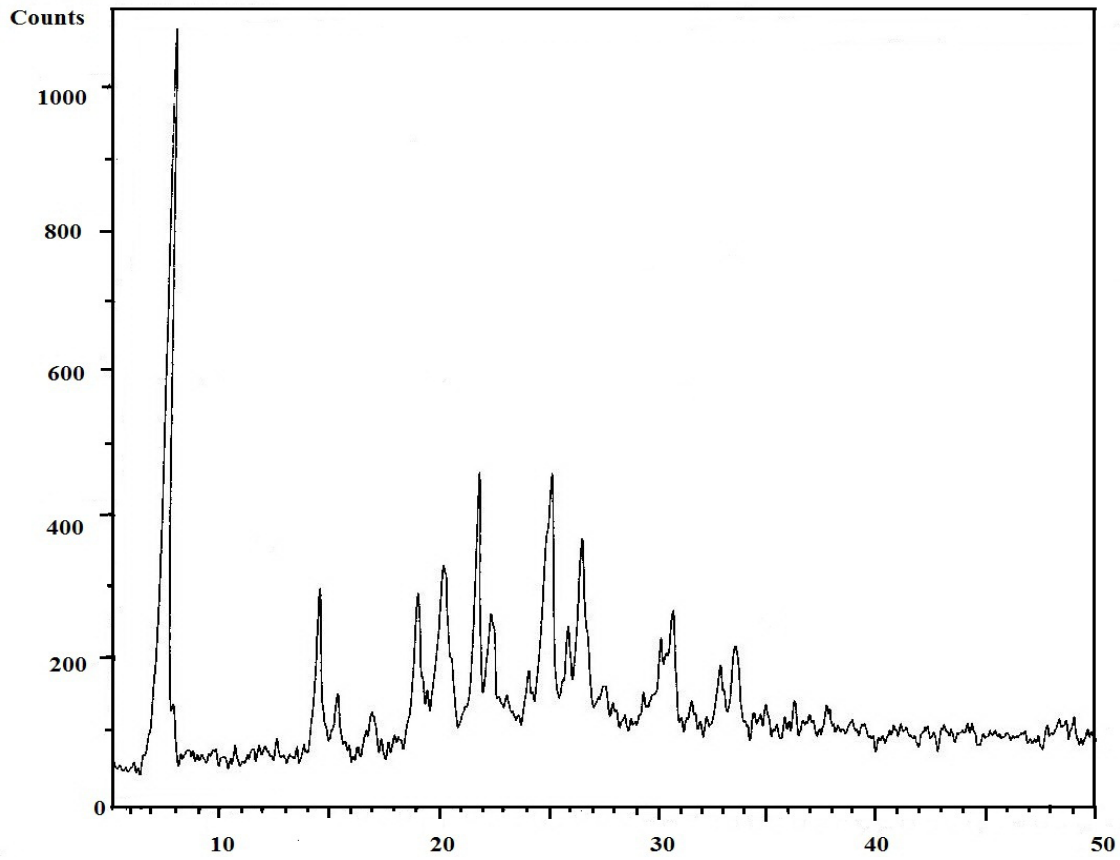

Fig. 15. X-Ray Diffraction pattern of orthorhombic DPC.

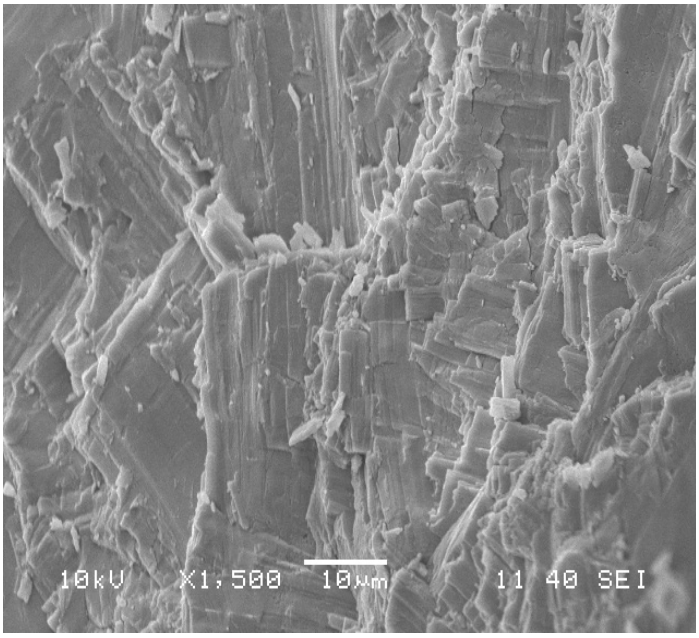

Photo. 1. SEM micrograph for an orthorhombic surface of DPC crystal sample (Magnification X = 1500).

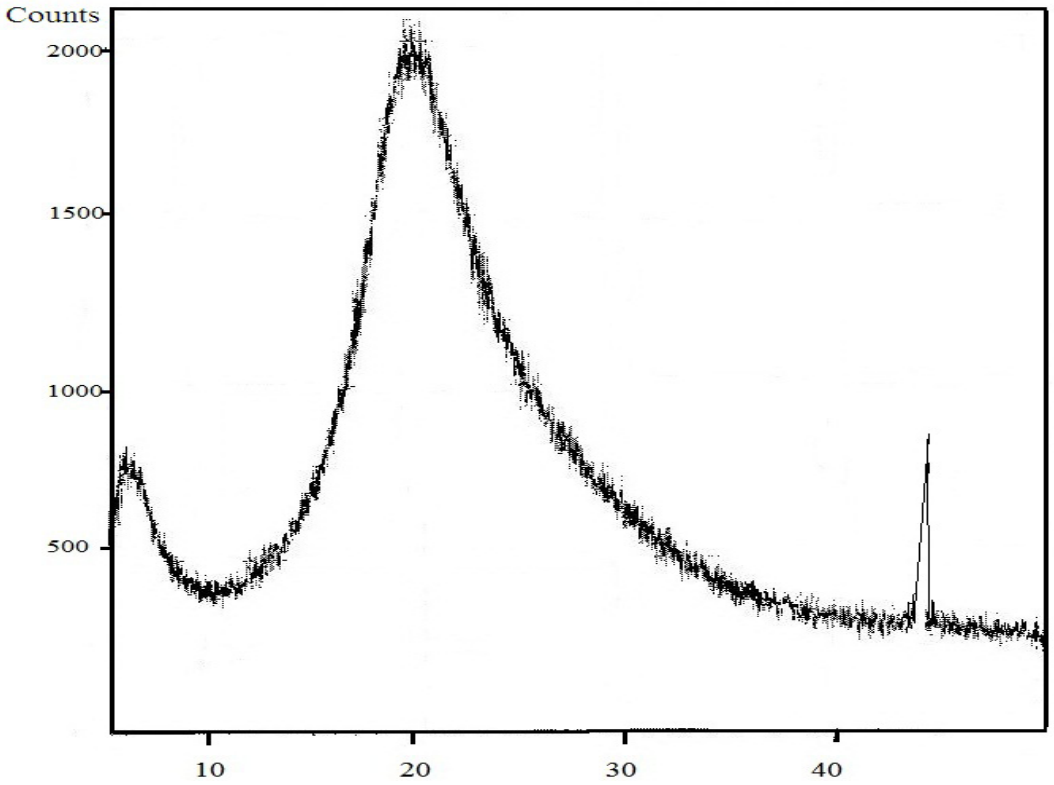

Fig. 16. X-Ray Diffraction pattern of amorphous DPC.

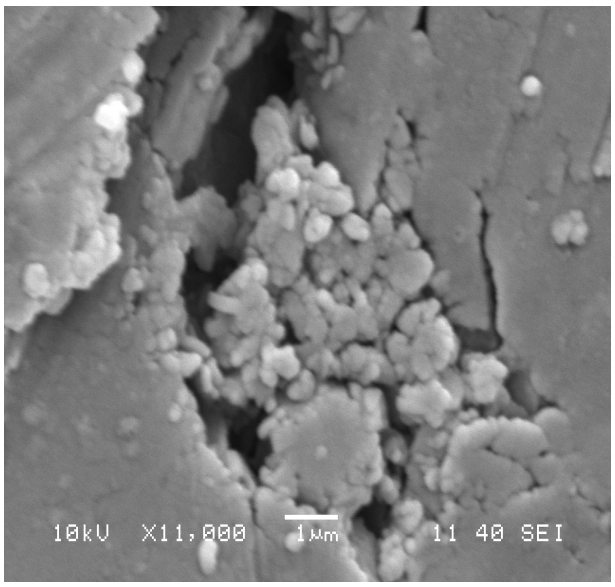

Photo. 2. SEM micrograph for an amorphous sample of DPC(Magnification X = 11000).

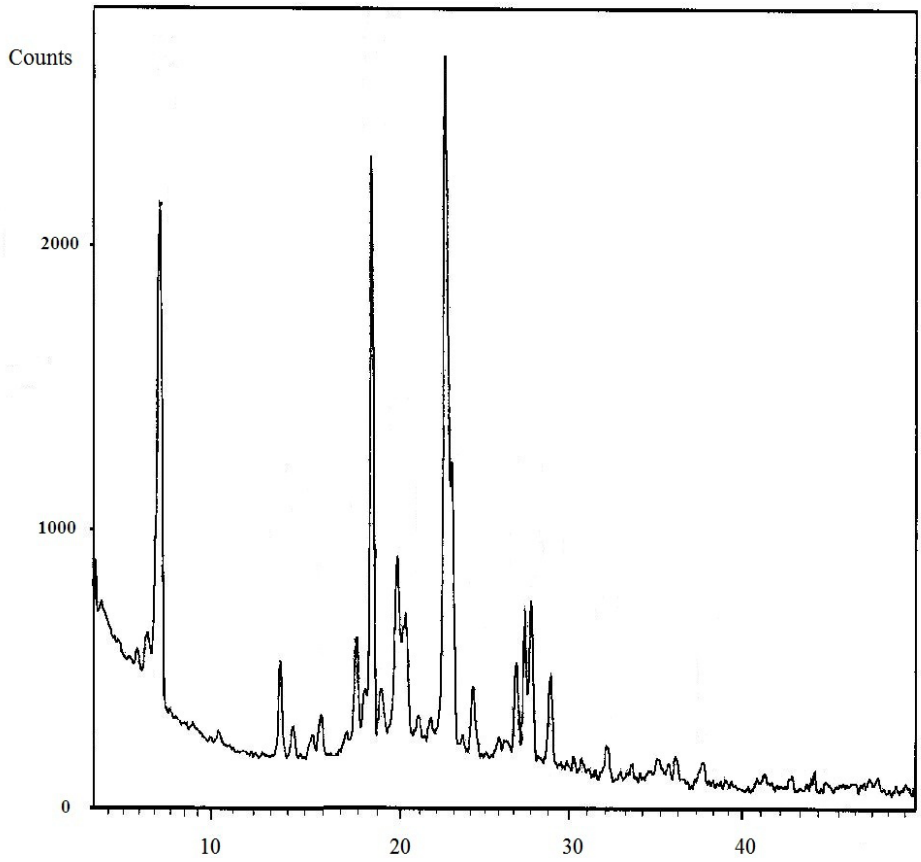

Fig. 17. X-Ray Diffraction pattern of triclinic LiDPC.

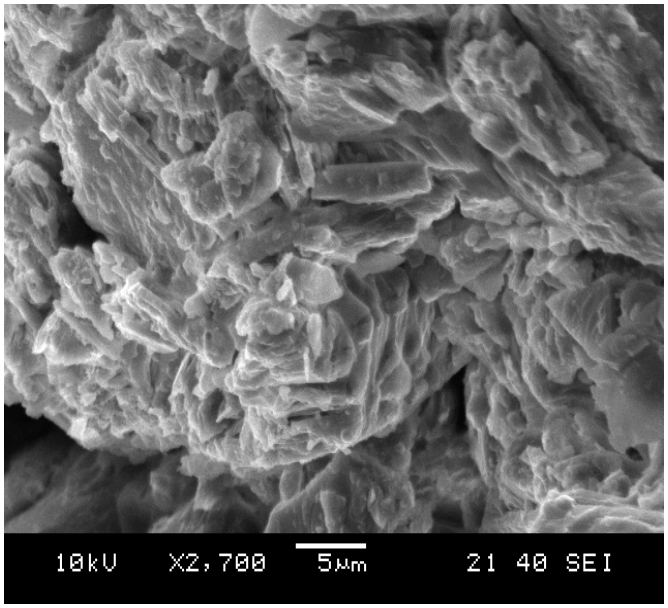

Photo. 3. SEM micrograph for a triclinic surface of LiDPC crystal sample (Magnification X = 2700).

worthily to go on new set of measurements of the physical features of LiDPC complex to find out new properties associated with it.

Conclusion

The results of study on the LiDPC new complex show several conclusions could be derived, and taken into consideration:

1. Thermal analysis (TGA and TMA) shows a weight loss 4.1% and shrinkage at 77 ^{o}C, changes to a fast shrinkage above 80 ^{o}C with a shrinkage coefficient 47.3 µm/^{o}C. The shrinkage phenomenon in LiDPC is found to be time dependent and the activation energy for the isothermal process is calculated and equal to 0.39 eV.
2. Mass and NMR analysis beside the photos of SEM for LiDPC organic complex confirm and support what is obtained by X-ray pattern. This indicates that introducing Li^{+} into DPC molecule leads to a new organic metal complex compound accompanied by changes in the thermal and crystal structure.
3. The current-voltage characteristics for LiDPC for different layers of thickness ranged from 150 to 1000 µm have been studied to obtain (V_C) and (V_b).
4. Heating effect of LiDPC samples shows a clear change in electric-current behavior near T_C = 60 ^{o}C.

Acknowledgements

The authors acknowledge Prof. Dr. Sayed Taha, Professor in Faculty of Science, El-Fayoum University for his assistance, support, useful discussions, comments and encouragement during this study.

References

1. H Assi, G Mouchaham, N Steunou , T Devic, C Serre, *Chem. Soc. Rev.* **11**(46),3431(2017).
2. B Marco, D Cortizo-Lacalle, I Perez-Miqueo, Giovanni Valenti, *Angew Chem. Int. Ed*. **56**(24), 6946(2017).
3. T Hammad, F El-kabbany and Y Badr, *physica status solidi* (a) **95**,121 (1986).
4. F El-Kabbany, W Badawy, E El-Khwas, and N Taher, *J Mater Sci* **23**,776 (1988) .
5. F El-Kabbany, S Taha, M Hafez, *Spectrochimica Acta* (A) **128**, 481(2014).
6. F El-Kabbany, S Taha, A Shehap and M El-Naggar, *J. Phys.Chem.Solids* **59**(9), 1619(1988) .
7. F El-Kabbany, S Taha, F Mansey, A Shehap and M Yousef , *J.Phys.Chem.Solids* **58**, 449(1997).
8. F El-Kabbany, S Taha, F Mansey and A Shehap, *Infrared physics & Technology* **38**, 169(1997).
9. C.J. De Ranter, N.M. Blaton, O.M. Peeters, *Acta Cryst.* B **35** (5), 1295(1979).
10. K Vijayakumar, RL Rengarajan, R Radhakristinan and A Vijaya Anand, *Pharacognosy Magazine,* **14** (53), 4 (2018).
11. C Londolani, J Sekomeng, Fanyana, J Micheal, and E Vusumzi, *Bioinorganic chemistry and application* Article ID 6171906, 2018 (2018)14 pages.
12. F El-Kabbany, S Taha, and M Hafez, *Spectrochimica Acta (*A), **111**,252 (2013) .
13. F El-Kabbany, S Taha , M Hafez , *Spectrochimica Acta* (A), **78** (3), 981(2011).
14. F El-Kabbany, S Taha , M Hafez , *J.Am.Sci.* **6** (8), 271(2010).
15. F El-Kabbany, S Taha , M Hafez , *Thermochimica Acta,* **510**,122 (2010) .
16. F El-Kabbany, S Taha , M Hafez , *J.Am.Sci*.**6** , 278(2010).
17. R Hoffmann , *Angew Chem. Int. Ed. Engl.* **26**, 846 (1987).
18. K. Yoshihito , R. Mann Kent , L. Miller Larry , L. Exstrom Christopher, *J. Am. Chem. Soc.* **120** (3), 589(1998).
19. M A Rawashleh-Omary, M A Omary, J P Fackler, *J. Inorganica Chimica Acta* **334**, 376 (2002).
20. F El-Kabbany, S Taha, M Hafez, N R Abdel Aziz, *Journal of Molecular Structure* **1092**, 113 (2015).
21. R Kamel, D. *Sc. Thesis,* Cairo University (1968).
22. R. Kamel and E. A. Attia, *Acta Met.* **9**, 1047 (1961).
23. J J O'DWYER The theory of Electrical Conduction and Breakdown in Solid Dielectrics", Oxford University Press, 427(1973).
24. N Klein and E Bursten, *J. Applied Physics,* **40**, 2728 (1969).
25. J J O'DWYER, *J. Phys. Chem. Solids* **28**, 1137 (1967).
26. C M Osburn and D W Ormond, *J. Electrochem. Soc.* **119** (5), 597(1972).
27. J J O'WYER "The theory of Electrical conduction and Breakdown in solid Dielectrics", Clarendon Press, Oxford, 219 (1973).

28. P Goldberg and J W Nickerson, *J.App.Phys.* **34**, 1601(1963).

29. N A Vlasenko and A N Gergell. *Phys.Status. Solidi* **26** K 77(1968).

30. P Gleichauf, *J.Appl. Phys.* **22**, 766 (1951).